COMPARATIVE STUDY ON CONTINUOUS STEEL-CONCRETE COMPOSITE BEAMS WITH NORMAL AND STEEL FIBER REINFORCED CONCRETE SLAB

T. YODA[1*†], W. LIN[1], N. TANIGUCHI[2], H. KASANO[1], L. HEANG[1], and H. GE[1]

[1]*Department of Civil and Environmental Engineering, Waseda University, Japan*
[2]*Department of Civil and Environmental Engineering, Maebashi Institute of Technology, Japan*

ABSTRACT

This paper describes the performance of composite steel and concrete beams subjected to negative bending moment. Static loading tests were performed on four overturned specimens. Two of the specimens are using SFRC as the concrete slab while the other two are using plain concrete as the slab. Two different types of shear connectors, including shear studs and PBLs, are used in the test specimens. Drying shrinkage of the concrete, load versus mid-span deflection, load carrying capacities, crack formation and its developing process were measured and studied. The results demonstrated that the application of SFRC would not only increase the initial cracking load, but also restrict the crack propagation in the service lifetime, and then the crack widths can be controlled appropriately. The use of steel fibers can improve the performance of the composite beams in the service load stage and the effects on the ultimate load stage of the composite beams are dependent on the shear connectors.

Keywords: SFRC; steel-concrete composite beams; hogging moment; shrinkage.

1. INTRODUCTION

Composite steel and concrete structures have been used extensively in both building and bridge structures due to the benefits of combining the advantages of component materials and obtaining efficient lightweight structural members. For continuous composite girders, negative bending moment acting on the support regions will generate tensile stresses in the concrete slab and compressive stresses in the lower steel profile. As a result, the mechanical behavior of these beams is strongly nonlinear even for low stress levels, due not only to the slip at the beam-slab interface, but also to cracking in the slab, which generally has shortcomings in view of durability and service life of the structures (Manfredi et al. 1996, and Ryu et al. 2005). The existing research results indicate that the SFRC has relatively high flexural strength (Uygunoglu 2008), modulus of elasticity (Pawade et al. 2011), and behaves well for long term behavior and durability performance (Vairagade et al. 2012) in

* Corresponding author: Email: yoda1914@waseda.jp

† Presenter: Email: yoda1914@waseda.jp

comparison with the normal concrete. Therefore, the use of SFRC could be a solution for improving the mechanical performance of the composite steel-concrete beams under negative bending moment.

A series of experimental studies were performed recently on steel-concrete composite beams subjected to hogging moment to study their fatigue loading behavior (Lin et al. 2013a, 2013b), static loading behavior (Lin et al. 2011), and hammer test behavior (Lin et al. 2013c), but no detailed results were reported on the use of SFRC in composite beams under negative bending moment. On this background, this paper deals with the results of a series of experimental work to make comparative study on composite beams with normal concrete and steel fiber reinforced concrete slab. This study keeps a watchful eye on the problems involving on SFRC on the beam stiffness, initial cracking load, ultimate load carrying capacity, crack formation and propagation on the concrete slab, as well as the slip development process on the steel-slab interface.

2. EXPERIMENTAL PROGRAMME

2.1. Test specimens

Four overturned simply supported steel-concrete composite beams CB-1 (normal concrete and stud connectors), CB-2 (normal concrete and PBLs connectors), CB-3 (SFRC and stud connectors) and CB-4 (SFRC and PBLs connectors) were tested under concentrated load in mid-span, which were used to simulate the support regions of continuous composite steel and concrete beam. Sketch of the steel fibers used in this study is shown in **Figure 2**. Each of the specimens was 4.6m in length and was simply supported at a span of 4m. The concrete slab thickness was 250mm with a width of 800mm. Vertical stiffeners were welded at supports, loading points to prevent shear buckling failure and crippling of the web before flexural failure. The typical geometry and design details of test specimen are shown in **Figure 1**.

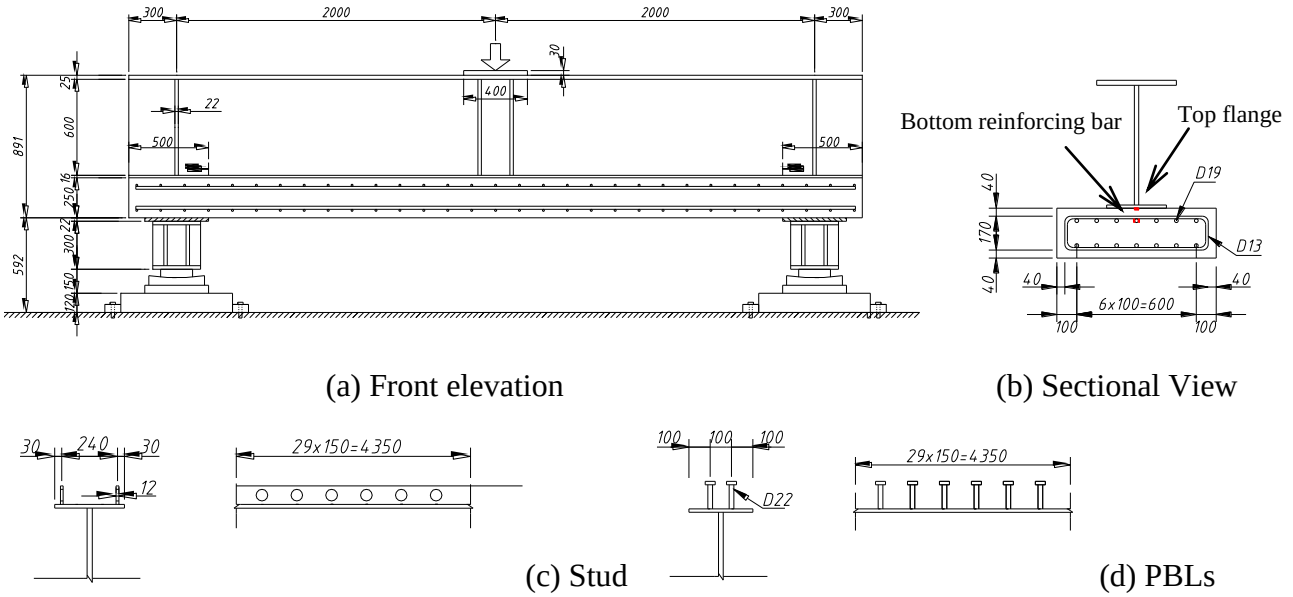

(a) Front elevation (b) Sectional View

(c) Stud (d) PBLs

Figure 1 Dimensions of the test specimen (unit: mm)

2.2. Instrumentation

12 linear variable differential transducers (LVDTs) were used to measure the vertical deformation at the mid-span and support locations. Strain gauges were used to measure the strain in the steel web, upper and lower steel flanges, concrete slab surface in key sections as well as the reinforcing bars and the shear studs. Besides, π-gauges for measuring the crack width on the concrete slab were also employed in the test.

2.3. Test set-up and loading procedure

The 5000kN loading capacity equipment was used in the experiment to apply a point load in the mid-span of the overturned composite beam. The test specimen was supported by a roller system at two ends, as shown in **Figure 3**. After the drying shrinkage had stabilized, pre-loading was applied to check the reliability of the measuring equipments and the stability of the test specimens. The negative bending load was applied by static loading with unloading process at the levels 200 (initial cracking load), 400, 700(stationary cracking load) and 1300kN with loading rates of 0.001mm/s, 0.0015mm/s, 0.002mm/s, and 0.003mm/s, respectively. Displacement control was used in the tests with a loading rate of 0.004mm/s for the subsequent experiment. The loading was terminated when either the maximum stroke of the jack was reached or the load capacity of the test specimen dropped significantly.

Figure 2 Sketch of the steel fibers

Figure 3 Static loading test set-up

3. RESULTS AND DISCUSSION

3.1. Compressive strength and shrinkage of concrete

Concrete cylinders of 10cm (diameter) ×20cm (height) were prepared for compression tests during casting of the concrete slab for each specimen. Seven days compressive strengths of normal concrete were 29.7MPa, 30.8MPa for CB-1 and -2, which were a little bit smaller than those of CB-3 and -4 with the compressive strengths of 32.8MPa and 32.4MPa, respectively. The results seem to indicate that the use of steel fibers can slightly enhance the compressive strengths of the concrete. Similar tendency was also found for 28 days compressive strengths of the concrete, as shown in **Table 1**.

Table 1 Test compressive strength.

Specimen	Design strength (N/mm^2)	Comprehensive strength (MPa)	
		7 days	28 days
CB-1	27	29.7	36.0
CB-2	27	30.8	35.9
CB-3	27	32.8	38.2
CB-4	27	32.4	38.7

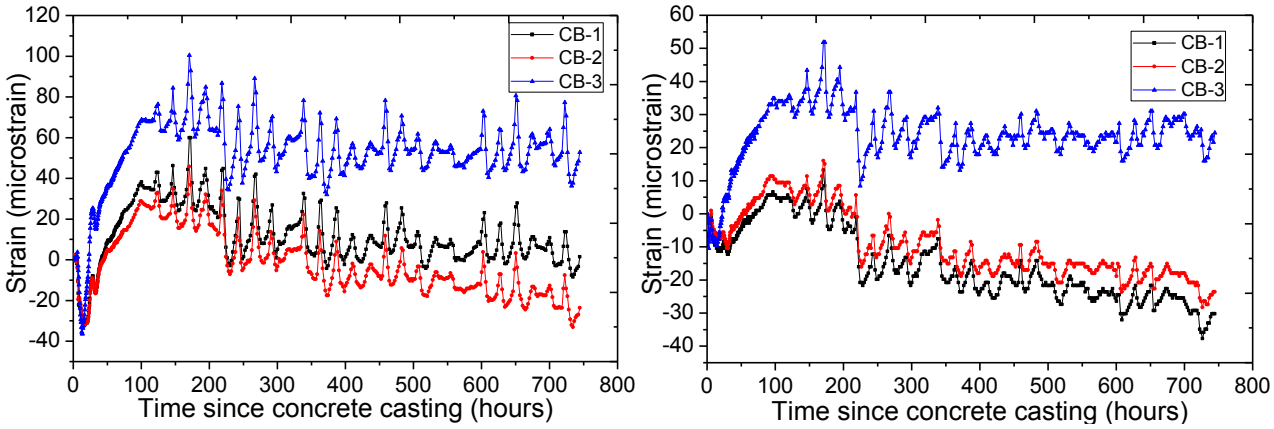

(a) Bottom reinforcing bars (b) Top flange of the steel girder

Figure 4 Strain changes in reinforcing bars and steel girder

Concrete shrinkage plays a major role in crack control and the service load behavior of concrete members. In order to compare the shrinkage of the normal concrete and SFRC used in this study, strain in reinforcing bars and top flange of the steel girder during 30 days (around 750 hours) after concrete casting was measured in CB-1, -2 and -3. Strain gauges were arranged on the top reinforcing bars, bottom reinforcing bars and top flange of the steel girder at the mid-span section, respectively, as shown in Figure 1(b). The results shown in **Figure 4** clearly indicate that the strain in reinforcing bars increased rapidly during the first 5 days for both normal concrete and SFRC, which might be due to swelling of the concrete. As 30kg/m^3 of swelling agent was added to the concrete mix of the SFRC, the shrinkage in CB-3 was not so serious like CB-1 or -2. It can be found that after the peak, the tension strains in reinforcing bars and top flange of the steel girder in CB-1 or -2 kept decreasing as the time went on, then initial cracks might appear on the rebar-concrete interface and steel-slab interface. On the contrary, although strain decreasing was also observed in CB-3 after the peak, the vibration of the strain is relative small and the strain-time response curve is relatively stable. Therefore, to the practical engineering structures, the shrinkage of SFRC can be controlled appropriately by using the swelling materials.

On the other hand, according to the strains measured in bottom layer reinforcing bars as shown in **Figure 4** (a), the maximum shrinkage was observed in CB-2. This is due to the total contact surface between PBL and concrete is 1.45×10^6mm^2, which is about three times of the contact area (5.39×10^5mm^2) between shear stud and surrounding concrete. Besides, as concrete goes through the holes, the PBLs could resist higher internal force caused by shrinkage of the concrete in comparison

with the stud connectors, resulting in relatively small strain in the top flange of the steel girder in CB-2 compare with CB-1, as shown in **Figure 4**.

3.2. Load-deflection response and load carrying capacities

The comparison of load-vertical displacement curves between CB-1, CB-2, CB-3, and CB-4 is illustrated in **Figure 5**. The displacement was taken at mid-span of the test specimen. The results indicate that application of SFRC could enhance the rigidity of composite beam in the initial stage (≤1250kN, as shown in **Figure 5**(a)), this might be due to the two reasons. Firstly, the use of steel fibers enhanced the tensile strength of the concrete and was useful for controlling the crack width. Secondly, the use of swelling materials restrained the occurrence of the initial cracks, as can be confirmed in **Figure 5**. But thereafter, there was no obvious difference. It is very interesting that the SFRC had different effects on the ultimate loading capacity of composite beams with different shear connectors. For composite beams using studs as shear connectors, the ultimate loading capacity of CB-3 was enhanced in comparison with that of CB-1; however, for composite beams using PBLs as shear connectors, the load carrying capacity of CB-4 was smaller than that of CB-2. Therefore, the effect of SFRC on the load carrying capacity of composite beams under hogging moment is related to the shear connectors. In addition, comparison of specimens indicates that the displacements of CB-2 and CB-4 become a little less at around 1000kN, this is presumably because of the PBL dowels affects the rigidity of the entire girder when cracking has progressed to a certain extent.

Table 2 shows the loading capacity of the test specimens. The initial cracking load calculated with reference to the slab exhibiting maximum negative moment of composite section under elastic state as shown in **Table 2**, were always larger than experimental values, which indicates that the real initial cracking load is very small and the structure will be in highly nonlinear even under relatively low load levels. The fourth column of **Table 2** presents the ratio between the theoretical and experimental initial cracking load, which indicates that the application of SFRC in CB-3 and CB-4 was useful for enhancing the initial cracking load in comparison with that of CB-1 and CB-2. The experimental yielding moment results are nearly equal but larger than those of theoretical predictions determined by AASHTO LRFD (2007), which might be due to ignoring the tension stiffening effect of the cracked concrete when calculating the beam yield moment. The comparison between the ultimate loads predicted experimentally and the theoretical values determined by the code is also given. The ultimate pure bending moments, $M_{u,e}$ is calculated following the procedure for computing the plastic bending moment of composite sections under negative moment specified in Appendix D6.1 of AASHTO LRFD (2007). Because of the restriction of the loading device (maximum loading capacity is 5000kN), the experiments were stopped at around 4000kN, and the real load carrying capacities of the specimens are assumed to be a little bit higher than this value. Even so, it is found that in all cases the theoretical prediction underestimates the test loading capacity, and the minimum deviation is about 28%, which indicates that the current AASHTO-LRFD specification is conservative in predicting the ultimate loading capacity of

composite beams under hogging moment. This could be caused by the neglect of the strain hardening of structural steels and reinforcements.

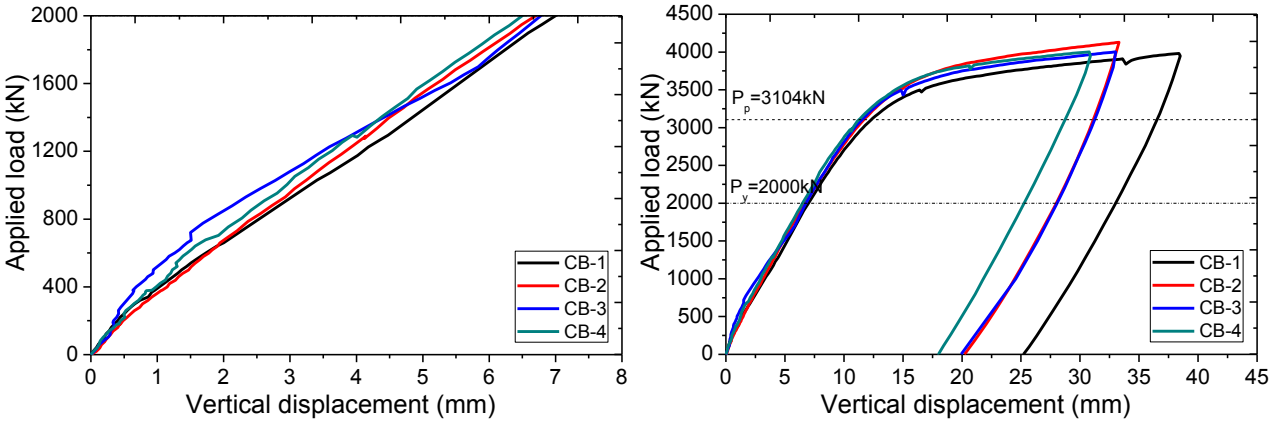

(a) P<2000 kN (b) whole loading process

Figure 5 Load-vertical deflection response of test specimens

Table 2 Load carrying capacity of the test specimens

Specimen No	Initial cracking moment (kN·m)			Yielding moment (kN·m)			Ultimate bending moment (kN·m)		
	$M_{c,e}$	$M_{c,t}$	$M_{c,e}/M_{c,t}$	$M_{y,e}$	$M_{y,t}$	$M_{y,e}/M_{y,t}$	$M_{u,e}$	$M_{u,t}$	$M_{u,e}/M_{u,t}$
CB-1	200	269	0.74	2234	2000	1.12	3981	3104	*1.28*
CB-2	120	269	0.45	2346	2000	1.17	4128	3104	*1.33*
CB-3	241	277	0.87	2458	2000	1.23	4003	3104	*1.29*
CB-4	260	279	0.93	2632	2000	1.32	4002	3104	*1.29*

Note: $M_{c,e}$ and $M_{c,t}$= Initial cracking bending moment from experiments and theoretical calculation; $M_{y,e}$, and $M_{y,t}$= Yielding moment from experiments and theoretical calculation; $M_{u,e}$ and $M_{u,t}$=ultimate bending moment from experiments and theoretical calculation, respectively.

3.2.1. Load-crack width response

Initial crack formation, crack width development during the loading process and distribution on the concrete slab were recorded by using 14 π-gauges on the top surface of the concrete slab. Numbers and locations of π-gauges in the experiments were shown in **Figure 6**.

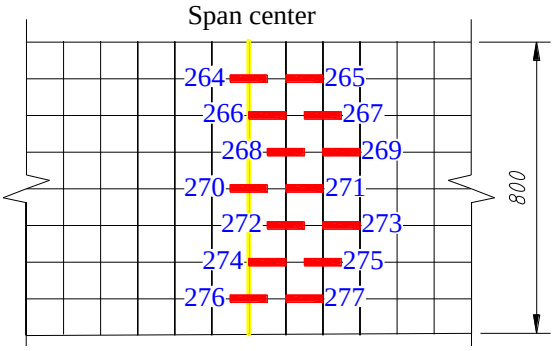

Figure 6 Arrangement of π gauges in test

As mentioned earlier, the negative bending load was applied by static loading with unloading process at the levels 200, 400, 700 and 1300kN before the final loading test was performed. The crack width of CB-1 and -3 during the loading process of 0-700kN was illustrated in **Figure 7** and **Figure 8**. For CB-1, it can be found that when the load was increased to 200kN, the crack width suddenly increased, indicating the formation of the initial crack. The maximum crack width (gauge numbered 265) increased suddenly to 0.25mm, which could affect on the serviceability of the

composite beam. On the contrary, the results shown in **Figure 8** demonstrate that the crack width of SFRC increased slowly with the load increase, and no "sudden increase of crack width" was observed. In order to confirm the affects of steel fibers in controlling the crack width, the average values of the crack width was compared between CB-1 and CB-3, as shown in **Figure 9** (a). The comparison indicates that for stud specimen, the application of SFRC would not only increase the initial cracking load, but also could limit the crack propagation, and relatively small crack width was observed in CB-3 in comparison with that of CB-1. Sudden increase of the crack width was observed in CB-1 (often referred to as crack jump); on the contrary, moderate growth of the crack width was observed in CB-3. Similar effects of SFRC were also observed in PBL specimens, as shown in **Figure 9 (b)**. Therefore, the crack width control effect of SFRC was confirmed in the test.

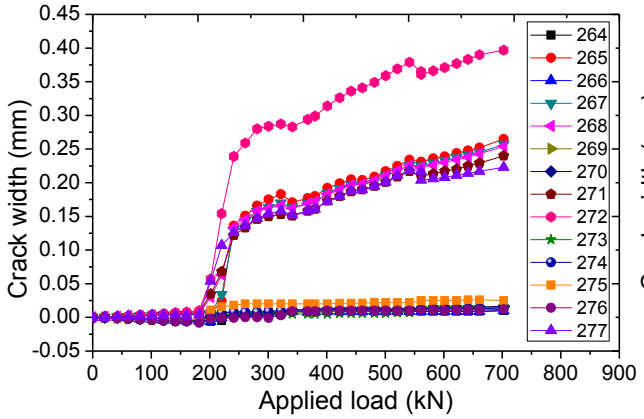

Figure 7 Load-crack width relationship in CB-1

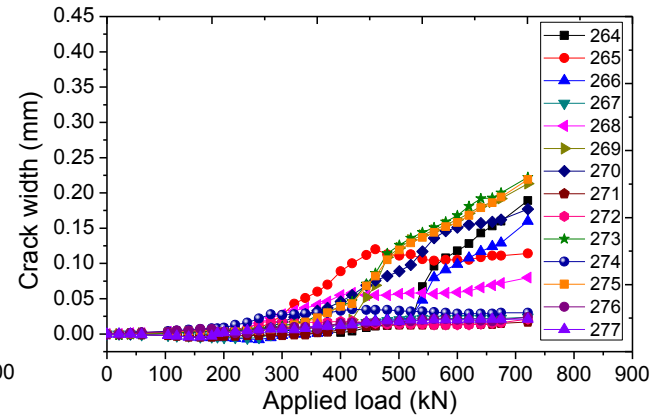

Figure 8 Load-crack width relationship in CB-3

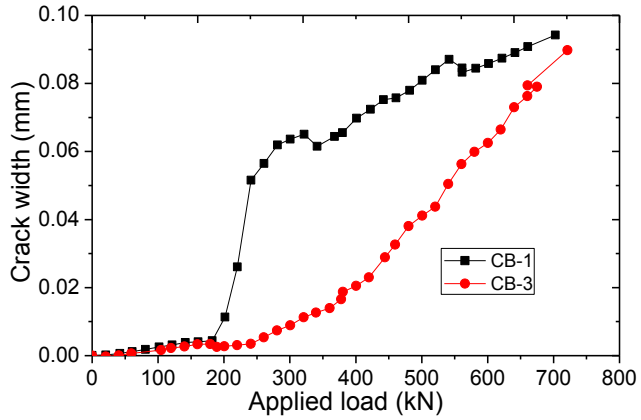

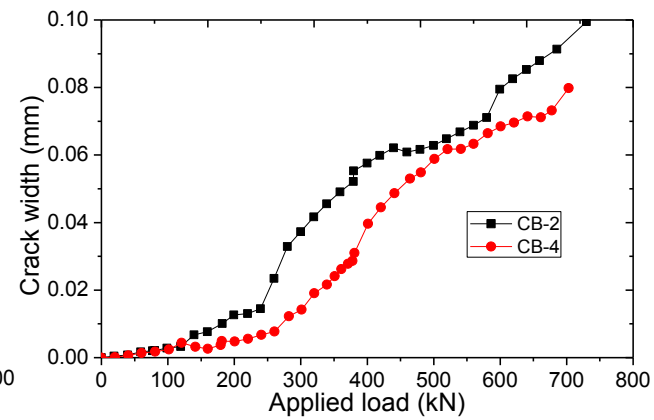

(a) Crack width development in CB-1 and CB-3 (b) Crack width development in CB-2 and CB-4

Figure 9 Crack width in specimens with normal concrete and steel fiber reinforced concrete

4. CONCLUSIONS

Static loading tests were performed on four steel-concrete composite beams with normal concrete slabs, SFRC slabs, and different types of shear connectors including PBLs and shear studs. Detailed results in shrinkage test as well as the static loading tests involving load-displacement response, crack formation and development process were measured carefully and reported in this paper. From

the present results, the following conclusions and recommendations deserving priority are made:

(1) The shrinkage in SFRC is less serious than that of normal concrete due to the use of the swelling materials, and the shrinkage of steel fiber reinforced concrete can be controlled approximately. Shrinkage in PBL specimens is remarkable relative to stud specimens, due to the larger contact area between the PBL and surrounding concrete.

(2) The specimens with steel fiber reinforced concrete have relatively large initial cracking load. The effects of the SFRC on the ultimate load carrying capacity of the steel-concrete composite beam also depend on the shear connectors applied on the steel-slab interface. Besides, the current AASHTO-LRFD specification is conservative in calculating the ultimate load carrying capacity of composite beams under hogging moment.

(3) The results indicate that for composite beams subjected to hogging moment, inclusion of steel fibers in the concrete slab would not only increase the initial cracking load, but also could limit the crack propagation and crack width. Therefore, the crack width control effect of SFRC was confirmed in the tests.

5. ACKNOWLEDGMENTS

The financial support for the experimental work sponsored by Ministry of Land, Infrastructure, Transport and Tourism of Japan is gratefully acknowledged.

REFERENCES

AASHTO (2007): AASHTO LRFD Bridge Design Specifications, Washington, DC.

Lin, W., Yoda, T., and Taniguchi, N. (2013a). ‘‘Fatigue Tests on Straight Steel-Concrete Composite Beams Subjected to Hogging Moment.’’ Journal of Constructional Steel Research, Vol. 80, pp. 42-56.

Lin, W., Yoda, T., Taniguchi, N., Kasano,H, and He, J. (2013b). ‘‘Mechanical Performance of Steel-Concrete Composite Beams Subjected to Hogging Moment.’’ Journal of Structural Engineering, ASCE. (Accepted, in print)

Lin, W., and Yoda, T. (2011). “Mechanical Behaviour of Composite Girders Subjected to Hogging Moment: Experimental Study.” Journal of Japan Society of Civil Engineers, Ser. A1 (Structural Engineering & Earthquake Engineering (SE/EE)) JSCE, 67(3), pp. 583-596.

Lin, W., and Yoda, T. (2013c). ‘‘Experimental and Numerical Study on Mechanical Behavior of Composite Girders under Hogging Moment.’’ International Journal of Advanced Steel Construction. 9(4).

Manfredi, G., Fabbrocino, G., and Cosenza, E (1996). Modeling of steel-concrete composite beams under negative bending. Journal of Engineering Mechanics-ASCE. 125(6), pp.654-62

Pawade, P.Y., Pande, A.M., and Nagainaki, P.B(2011). Effect of Steel Fibers on Modulus of Elasticity of Concrete, International Journal of Advanced Engineering Sciences and Technologies. 7(2), pp.169-177.

Ryu, H.K, Chang, S.P., Kim, Y.J. and Kim, B.S (2005). Crack control of a steel and concrete composite plate girder with prefabricated slabs under hogging moments, Engineering Structures. 27(11), pp.1613-24.

Uygunoglu, T (2008). Investigation of Microstructure and Flexural Behavior of Steel Fiber Reinforced Concrete, Journal of Materials and Structures. Vol. 41, pp.1441-1449.

Vairagade, V.S., Kavita S. Kene, K.S., and Patil, T.R (2012). Comparative study of steel fiber reinforced over control concrete. International Journal of Scientific and Research Publication. 2(5), pp.1-3.